ON THE STABILITY OF AXISYMMETRIC COMPRESSIBLE, VORTICAL NON-ISENTROPIC FLOW

L. M. B. C. Campos[a,*], A. C. Marta[a]

[a]*Center for Aeronautical and Space Science and Technology, IDMEC/LAETA,
Instituto Superior Técnico, Universidade de Lisboa, Av. Rovisco Pais 1, 1049-001 Lisboa, Portugal*

Abstract

The noise of jet and rocket engines involves the coupling of sound to swirling flows and to heat exchanges leading in the more complex cases of triple interactions to acoustic-vortical-entropy (AVE) waves. The present paper presents the derivation of the AVE equation for axisymmetric linear non-dissipative perturbations of a compressible, non-isentropic, swirling mean flow, with constant axial velocity and constant angular velocity. The axisymmetric AVE wave equation is obtained for the radial velocity perturbation, specifying its radial dependence for a given frequency and axial wavenumber. The AVE wave equation in the case of zero axial wavenumber has only one singularity at the critical radius, where the isothermal Mach number for the swirl velocity is unity. The exact solution of the AVE wave equation is obtained as series expansions of Gaussian hypergeometric type valid inside, outside and around the critical layer. Using polarization relations among wave variables specifies exactly the perturbations of: (i,ii) the radial and azimuthal velocity; (iii,iv) pressure and mass density; (v,vi) entropy and temperature. It is shown that the dependence of the AVE wave variables on the radial distance can be: (a) oscillatory with decaying amplitude; (b) monotonic with increasing amplitude. The case (b) of AVE wave amplitude increasing monotonically with the radial distance applies if the frequency times a function of the adiabatic exponent is less than the vorticity (or twice the angular velocity). In the opposite case (a) the oscillatory nature of acoustic waves predominates over the tendency for monotonic growth of vortical perturbations. Associating sound with stable potential flows and swirl with unstable vortical flows suggests a criterion valid in non-isentropic conditions, that is in the presence of heat exchanges, that is a condition for stable combustion in a confined space: the peak vorticity (multiplied by a factor of order unity dependent on the adiabatic exponent) should be less than the lowest or fundamental frequency of the cavity.

Keywords: aeroacoustics, absolute/convective instability, critical layers

1. INTRODUCTION

The noise of aircraft engines is a major limitation on airport operations, and the subject of ever more stringent certification rules, aiming to limit the total noise exposure as air traffic grows. The literature on aircraft usually considers purely acoustic waves, although coupling with other modes occur in: (i) inlet ducts due to the shear flow in the wall boundary layers; (ii) in turbine exhausts due to the downstream swirling flow; (iii) in the combustion chambers and other heat generation and exchange processes involving non-isentropic flows. In spite of the practical ubiquity of these phenomena, the present paper may be one of the first to consider the triple interaction of acoustic, vortical and entropy perturbations.

There are [1] three types of waves in a fluid in the absence of external restoring forces [2], namely: (i) sound waves that are longitudinal and compressive; (ii) vortical waves that are transversal, hence incompressible; (iii) entropy modes associated with heat exchanges, hence non-isentropic flow. The acoustic modes receive most attention because for an homogeneous uniform mean flow: (i) the acoustic modes satisfy the convected wave equation for uniform motion and the classical wave equation in a medium at rest [3]; (ii) by Kelvin circulation theorem the circulation along a loop convected with the mean flow is constant [4]; (iii) in homentropic conditions there are no entropy modes. The most general conditions for the existence of purely acoustic modes, decoupled from vortical-entropy modes, is a potential homentropic mean flow, that may be compressible, and leads to the high-speed wave equation [5] that reduces to the convected wave equation [6] in two cases: (i) uniform flow; (ii) low Mach number

---

*Corresponding author email: luis.campos@tecnico.ulisboa.pt

non-uniform flow. The presence of vorticity leads to acoustic-vortical-waves [7], in a compressible sheared [8] or swirling [9] mean flow. The present paper considers a further extension to acoustic-vortical-entropy waves that specify the stability of a compressible, vortical non-isentropic mean flow.

The present paper is about linear perturbations of a compressible, vortical, non-isentropic mean flow occupying all space, that may be designated acoustic-vortical-entropy waves. These perturbations determine the stability of the mean flow [10, 11] in this case the stability of a compressible, vortical, non-isentropic flow. The paper considers what possibly is the simplest case of acoustic-vortical-entropy (AVE) waves: (i) linear non-dissipative perturbations of an axisymmetric mean flow with uniform axial velocity and rigid-body swirl; (ii) the mean flow is compressible, vortical and non-isentropic allowing for the existence of AVE waves; (iii) the perturbations depend on time, axial and radial coordinates, but not on azimuthal angle; (iv) this allows for the fundamental axisymmetric mode, but excludes all non-axisymmetric azimuthal modes.

2. THE ACOUSTIC-VORTICAL-ENTROPY WAVE EQUATION

2.1. Compressible, vortical, non-isentropic flow of a perfect gas

The fundamental equations of fluid mechanics are written in cylindrical coordinates (r, φ, z) in axisymmetric form without φ-dependence $(\partial/\partial\varphi = 0)$:
(i) mass conservation:

$$\mathrm{D}\Gamma/\mathrm{d}t = -\Gamma \boldsymbol{\nabla} \cdot \boldsymbol{V} = -\frac{\Gamma}{r}\frac{\partial}{\partial r}\left(rV_r\right) - \Gamma\frac{\partial V_z}{\partial z}\,; \quad (1)$$

(ii) inviscid momentum:

$$\Gamma\left(\mathrm{D}V_r/\mathrm{d}t - r^{-1}V_\varphi^2\right) + \partial_r P \;=\; 0\,, \quad (2a)$$

$$\Gamma\left(\mathrm{D}V_\varphi/\mathrm{d}t + r^{-1}V_rV_\varphi\right) + r^{-1}\partial_\varphi P \;=\; 0\,, \quad (2b)$$

$$\Gamma\mathrm{D}V_z/\mathrm{d}t + \partial_z P \;=\; 0\,; \quad (2c)$$

(iii) energy:
$$\Gamma T\,\mathrm{D}S/\mathrm{d}t = 0\,; \quad (3)$$

(iii) state:

$$\mathrm{D}P/\mathrm{d}t = c^2\mathrm{D}\Gamma/\mathrm{d}t + \beta\mathrm{D}S/\mathrm{d}t\,; \quad (4)$$

where Γ is the mass density, P the pressure, $\boldsymbol{V}$ the velocity, T the temperature, S the entropy, the material derivative is denoted by

$$\mathrm{D}/\mathrm{d}t = \partial/\partial t + \boldsymbol{V}\cdot\boldsymbol{\nabla} = \partial/\partial t + V_r\partial_r + V_z\partial_z\,, \quad (5a,b)$$

and the equation of state in the form (6a) specifies the coefficients in (4),

$$P = P(\Gamma, S) : c^2 \equiv \left(\frac{\partial P}{\partial \Gamma}\right)_S,\ \beta = \left(\frac{\partial P}{\partial S}\right)_\Gamma, \quad (6a-c)$$

namely the adiabatic sound speed (6b) and the non-isentropic coefficient (6c). Chemical reactions are not considered explicitly and appear through the entropy coefficient.

In the case of a perfect gas, the equations of state (7a) and entropy (7b),

$$P = R\Gamma T,\quad S = C_V \log P - C_P \log\Gamma\,, \quad (7a,b)$$

involve the gas constant R and specific heats at constant volume C_V and pressure C_P that are related by the adiabatic exponent (8b),

$$R = C_P - C_V\,,\quad \gamma = \frac{C_P}{C_V}\,. \quad (8a,b)$$

From the entropy equation (7b) it follows

$$\mathrm{d}S = C_V\frac{\mathrm{d}P}{P} - C_P\frac{\mathrm{d}\Gamma}{\Gamma}\,, \quad (9a)$$

that the adiabatic sound speed (9b) is given by (9c),

$$\mathrm{d}S = 0 :\quad c^2 = \left(\frac{\partial P}{\partial \Gamma}\right)_S = \gamma\frac{P}{\Gamma} = \gamma RT\,. \quad (9b,c)$$

The non-isentropic coefficient (6c) may be calculated (10b) from the specific heat at constant volume (10a),

$$C_V = T\left(\frac{\partial S}{\partial T}\right)_\Gamma :\quad \beta = \frac{T}{C_V}\left(\frac{\partial P}{\partial T}\right)_\Gamma\,; \quad (10a,b)$$

in the case of a perfect gas (7a) follows (11a,b),

$$\beta = \frac{T}{C_V}R\Gamma = \frac{P}{C_V} = \frac{\gamma-1}{R}P\,, \quad (11a-c)$$

and also (11c) using (8a,b).

2.2. Linear perturbation of a uniform flow with rigid body swirl

The mean flow is assumed to consist (12a) of a uniform axial velocity plus a rigid body swirl,

$$\boldsymbol{V}_0 = \boldsymbol{e}_z U + \boldsymbol{e}_\varphi \Omega r\,,\quad \boldsymbol{\varpi} = \boldsymbol{\nabla}\times\boldsymbol{V}_0 = \boldsymbol{e}_z 2\Omega\,, \quad (12a,b)$$

so that the vorticity (12b) is twice the angular velocity. The linearised material derivative (5a) for the mean flow (12a) is

$$\mathrm{d}/\mathrm{d}t \equiv \partial/\partial t + \boldsymbol{V}_0\cdot\boldsymbol{\nabla} = \partial/\partial t + U\partial/\partial z\,. \quad (13)$$

Applying the fundamental equations to the mean flow (12a) it follows that: (i-ii) the mass density (1) and entropy (3) can depend only on the radius (14a,b); (iii)

there is a radial pressure gradient (2a) due to the centrifugal force (14c),

$$\rho_0 = \rho_0(r)\,,\ s_0 = s_0(r)\ :\quad p_0' \equiv \mathrm{d}p_0/\mathrm{d}r = \rho_0\Omega^2 r\,;$$
$$(14\mathrm{a}-\mathrm{c})$$

assuming a constant mass density (15a) leads to the pressure (15c) where (15b) is the pressure on axis,

$$\rho_0 = \mathrm{const}\,,\ p_{00} = p_0(0)\ :\quad p_0(r) = p_{00} + \frac{1}{2}\rho_0\Omega^2 r^2\,.$$
$$(15\mathrm{a}-\mathrm{c})$$

The sound speed (9c) and non-isentropic coefficient (11b) are given in the mean flow respectively by (16b) and (16c), where (9a) is the sound speed on the axis,

$$c_{00}^2 = \gamma\frac{p_{00}}{\rho_0}\ :\ [c_0(r)]^2 = c_{00}^2 + \frac{\gamma}{2}\Omega^2 r^2\,,\ \beta_0(r) = \frac{p_0(r)}{C_V}\,.$$
$$(16\mathrm{a}-\mathrm{c})$$

The entropy in the mean flow (17a),

$$s_0 = C_V \log p_0 - C_P \log \rho_0\,,\qquad (17\mathrm{a})$$

has radial gradient (17b),

$$s_0' = C_V\frac{p_0'}{p_0} = \frac{p_0'}{\beta_0} = C_P\frac{\Omega^2 r}{c_0^2}\,.\qquad (17\mathrm{b})$$

The linear perturbation of this mean flow is considered next.

The total flow is assumed to consist of the mean flow plus a perturbation depending on time t, radial r and axial z coordinate, but not on the azimuthal coordinate φ,

$$V_r(r,z,t) = v_r(r,z,t)\,,\quad V_\varphi(r,z,t) = \Omega r + v_\varphi(r,z,t)\,,$$
$$(18\mathrm{a,b})$$
$$V_z(r,z,t) = U + v_z(r,z,t)\,,\quad P(r,z,t) = p_0(r) + p(r,z,t)\,,$$
$$(18\mathrm{c,d})$$
$$\Gamma(r,z,t) = \rho_0 + \rho(r,z,t)\,,\quad S(r,z,t) = s_0(r) + s(r,z,t)\,.$$
$$(18\mathrm{d}-\mathrm{f})$$

Since the mean flow properties, that appear as coefficients in the linearisation, depend on r but not (z,t), the Fourier transform is made (19) with frequency ω and axial wavenumber k,

$$f(r,z,t) = \int_{-\infty}^{+\infty}\mathrm{d}k\int_{-\infty}^{+\infty}\mathrm{d}\omega\, e^{\mathrm{i}(kx-\omega t)}\tilde{f}(r,k,\omega)\,;\quad (19)$$

for example the linearised material derivative (13) leads (20a) to the frequency (20b) Doppler shifted by the axial mean flow,

$$\mathrm{d}/\mathrm{d}t \to -\mathrm{i}\omega_*\ :\quad \omega_* = \omega - kU\,.\qquad (20\mathrm{a,b})$$

Substituting (18a–f) in (1,2a–c,3,4) and linearising

leads to

$$\mathrm{i}\omega_* r\tilde{\rho} - \rho_0(r\tilde{v}_r)' - \mathrm{i}\rho_0 kr\tilde{v}_z = 0\,,\qquad (21\mathrm{a})$$

$$\mathrm{i}\rho_0\omega_*\tilde{v}_r + 2\Omega\rho_0\tilde{v}_\varphi + \Omega^2 r\tilde{\rho} - \tilde{p}' = 0\,,\quad (21\mathrm{b})$$

$$\mathrm{i}\omega_*\tilde{v}_\varphi - 2\Omega\tilde{v}_r = 0\,,\qquad (21\mathrm{c})$$

$$\rho_0\omega_*\tilde{v}_z - k\tilde{p} = 0\,,\qquad (21\mathrm{d})$$

$$\mathrm{i}\omega_*\tilde{s} = s_0'\tilde{v}_r = C_P\frac{\Omega^2}{c_0^2}r\tilde{v}_r\,,\qquad (21\mathrm{e})$$

$$\tilde{p} = c_0^2\tilde{\rho} + \beta_0\tilde{s}\,.\qquad (21\mathrm{f})$$

2.3. Wave equation for the radial velocity and polarization relations

Of the six variables in (21a–f) four $(\tilde{v}_r,\tilde{v}_\varphi,\tilde{\rho},\tilde{s})$ are expressible (21d,c,e,a) in terms of $(\tilde{p},\tilde{v}_r)$,

$$\tilde{v}_z = \frac{k}{\rho_0\omega_*}\tilde{p}\,,\quad \tilde{v}_\varphi = -\mathrm{i}\frac{2\Omega}{\omega_*}\tilde{v}_r\,,\quad \tilde{s} = -\mathrm{i}C_P\frac{\Omega^2}{c_0^2\omega_*}r\tilde{v}_r\,.$$
$$(22\mathrm{a}-\mathrm{c})$$
$$\tilde{\rho} = -\mathrm{i}\frac{\rho_0}{\omega_* r}(r\tilde{v}_r)' + \frac{k^2}{\omega_*^2}\tilde{p}\,.\qquad (22\mathrm{d})$$

Substituting (22c,d) in (21f) leads to

$$\mathrm{i}\tilde{p}\left(\omega_* - k^2 c_0^2/\omega_*\right) = \rho_0\left(\Omega^2 r + c_0^2/r\right)\tilde{v}_r + \rho_0 c_0^2\tilde{v}_r'\,,\ (23)$$

the pressure in terms of the radial velocity spectrum.

Substituting (22b,d) in (21b) leads to a relation between $\tilde{p}$ and $\tilde{v}_r$ distinct from (23), namely

$$\mathrm{i}\rho_0\left[\left(\omega_*^2 - 5\Omega^2\right)\tilde{v}_r - \Omega^2 r\tilde{v}_r'\right] = \omega_*\tilde{p}' - \frac{k^2\Omega^2 r}{\omega_*}\tilde{p}\,.\quad (24)$$

Substituting $\tilde{p}$ from (23) in (24) leads to the acoustic-vortical-entropy wave equation for the radial velocity perturbation spectrum,

$$c_0^2\tilde{v}_r'' + A\tilde{v}_r' + B\tilde{v}_r = 0\,,\qquad (25)$$

with coefficients

$$X \equiv 1 - k^2 c_0^2/\omega_*^2\ :\quad A = c_0^2/r + X\left[c_0^2/X\right]'\,,$$
$$(26\mathrm{a,b})$$
$$B = \left(\omega_*^2 - 5\Omega^2\right)X - k^2\Omega^2\left(\Omega^2 r^2 + c_0^2\right)/\omega_*^2 + X\left[\left(\Omega^2 r + c_0^2/r\right)/X\right]'\,.$$
$$(26\mathrm{c})$$

In conclusion the axisymmetric compressive, vortical, non-isentropic perturbations of a uniform axial flow with rigid body swirl (12a), with frequency ω and axial wavenumber k, lead (19) to the acoustic-vortical-entropy wave equation (25) with coefficients (26a–c) satisfied by the radial velocity perturbation spectrum. The other wave variables are specified by the following polarization relations: (i–iii) the pressure (23), entropy (22c) and azimuthal velocity (22b) perturbation spectra; (iv–v) the axial velocity (22a) and mass density (22d)

perturbation spectra lead, by (23), respectively to (27a) and (27b),

$$\tilde{v}_z = -\mathrm{i}k \left[\left(\Omega^2 r + c_0^2/r \right) \tilde{v}_r + c_0^2 \tilde{v}_r' \right] / \left(\omega_*^2 - k^2 c_0^2 \right) , \tag{27a}$$

$$\mathrm{i}\tilde{\rho}/\rho_0 = \tilde{v}_r'/\omega_* + \tilde{v}_r/(\omega_* r) + k^2 \left[\left(\Omega r + c_0^2/r \right) \tilde{v}_r + c_0^2 \tilde{v}_r' \right] / \left(\omega_*^3 - k^2 c_0^2 \omega_* \right) . \tag{27b}$$

The temperature perturbation spectrum follows from the equation of state (7a),

$$R\tilde{T} = \frac{\tilde{p}}{\rho_0} - \frac{p_0}{\rho_0^2} \tilde{\rho} = \frac{\mathrm{i}c_0^2}{\omega_* \gamma} \left(\tilde{v}_r' + \tilde{v}_r/r \right) - \mathrm{i} \frac{\omega_* - k^2 c_0^2/\gamma \omega_*}{\omega_*^2 - k^2 c_0^2} \left[\left(\Omega^2 r + c_0^2/r \right) \tilde{v}_r + c_0^2 \tilde{v}_r' \right] ; \tag{28a, b}$$

using (27b) and (23).

3. MONOTONIC AND OSCILLATORY INNER AND OUTER SOLUTIONS

3.1. Condition separating oscillatory from monotonic radial dependences

If the axial wavenumber is not zero, the vanishing of (26a) introduces singularities in the AVE wave equation (25). The present paper concentrates in the simpler case of zero axial wavenumber (29a), that is neglecting axial dependence, there is (20b) no Doppler shift (29b) and the coefficients of the wave equation (26a–c) simplify respectively to (29d–f),

$$k = 0 \,, \; \omega_* = \omega \,, \; (c_0^2)' = \gamma \Omega^2 r \,, \; X = 1 : \; A = c_0^2/r + (c_0^2)' = \gamma \Omega^2 r + c_0^2/r \,, \tag{29a-e}$$

$$B = \omega^2 - 5\Omega^2 + \left(\Omega^2 r + c_0^2/r \right)' = \omega^2 - 4\Omega^2 + \gamma \Omega^2 - c_0^2/r^2 \,, \tag{29f}$$

where the radial dependence of the sound speed (16c) was used (29c). Thus the acoustic-vortical-entropy wave equation (25) for (29a–f) an axisymmetric mode of frequency ω simplifies to

$$c_0^2 \tilde{v}_r'' + \left(\gamma \Omega^2 r + c_0^2/r \right) \tilde{v}_r' + \left[\omega^2 + (\gamma - 4)\Omega^2 - c_0^2/r^2 \right] \tilde{v}_r = 0 . \tag{30}$$

The radial dependence of the sound speed (16b) is quadratic (31a),

$$[c_0(r)]^2 = c_{00}^2 \left[1 + (r/r_0)^2 \right] \,, \quad r_0 = (c_{00}/\Omega) \sqrt{2/\gamma} \,, \tag{31a, b}$$

with reference radius (31b). Substituting (31b) in the wave equation (30) leads to

$$r^2 \left(1 + r^2/r_0^2 \right) \tilde{v}_r'' + r \left(1 + 3r^2/r_0^2 \right) \tilde{v}_r' + \left\{ \left[(\omega/c_{00})^2 + (1 - 8/\gamma)/r_0^2 \right] r^2 - 1 \right\} \tilde{v}_r = 0 . \tag{32}$$

Using (29a) and (31a,b), the remaining wave variables are the azimuthal velocity (22b), mass density (27b), temperature (28a), entropy (22c) and pressure (23) specified respectively by (33a–e),

$$\tilde{v}_\varphi = -\mathrm{i}\frac{2\Omega}{\omega} \tilde{v}_r \,, \quad \tilde{\rho} = -\mathrm{i}(\rho_0/\omega) \left(\tilde{v}_r' + \tilde{v}_r/r \right) \,, \tag{33a, b}$$

$$\tilde{T}/T_0 = \left[(\gamma/c_0^2)\tilde{p} - \tilde{\rho} \right] / \rho_0 \,, \quad \tilde{s} = -\mathrm{i}\frac{2}{\omega} \frac{C_V r \tilde{v}_r}{r^2 + r_0^2} \,, \tag{33c, d}$$

$$\tilde{p} = -\mathrm{i}\frac{\rho_0 \gamma \Omega^2}{2\omega} \left[\left(r + 2r/\gamma + r_0^2/r \right) \tilde{v}_r + \left(r^2 + r_0^2 \right) \tilde{v}_r' \right] \,, \tag{33e}$$

in terms of the radial velocity perturbation spectrum.

The adiabatic exponent for a perfect gas is given by (34b) where (34a) is the number of degrees of freedom of a molecule,

$$N = 3, 5, 6 \; : \quad \gamma = 1 + \frac{2}{N} = \frac{5}{3}, \frac{7}{5}, \frac{4}{3} \,, \tag{34a, b}$$

namely: (i) three for monoatomic gas; (ii) five for a diatomic gas or polyatomic gas with molecules in a line; (iii) six for a three-dimensional polyatomic molecule. The reference radius (31b) corresponds to a ratio of the azimuthal velocity of the mean flow to the sound speed on axis given by

$$\frac{r_0 \Omega}{c_{00}} = \sqrt{\frac{2}{\gamma}} = \sqrt{\frac{2N}{N+2}} = \sqrt{\frac{6}{5}}, \sqrt{\frac{10}{7}}, \sqrt{\frac{3}{2}} \,, \tag{35}$$

that is of order unity and plays the role of swirl Mach number at the axis, bearing in mind that the sound speed (31a,b) is not constant. Using the sound speed (31a) at the critical radius (36a) leads to (36b),

$$c_0(r_0) = c_{00}\sqrt{2} \; : \quad r_0 \Omega = \frac{c_0(r_0)}{\sqrt{\gamma}} = \sqrt{RT_0(r_0)} = \bar{c}_0(r_0) \,, \tag{36a, b}$$

showing that the critical radius corresponds to azimuthal velocity equal to the isothermal sound speed, that is isothermal swirl Mach number unity. Since vortical modes are transversal and hence incompressible, the relevant sound speed and Mach number are isothermal. If the radius is small compared with the reference radius (37a), that is for small swirl isothermal Mach number, the wave equation (32) simplifies to (37b),

$$r^2 \ll r_0^2 \; : \quad r^2 \tilde{v}_r'' + r \tilde{v}_r' + \left(\chi^2 r^2 - 1 \right) \tilde{v}_r = 0 \,, \tag{37a, b}$$

that is a Bessel equation of order unity with radial wavenumber (38a),

$$\chi \equiv \kappa/r_0 \,, \quad \kappa^2 = \bar{\omega}^2 + 1 - 8/\gamma \,, \quad \bar{\omega} \equiv \omega r_0/c_{00} \,, \tag{38a-c}$$

where (38b) is the dimensionless radial wavenumber involving the dimensionless frequency (38c).

The Bessel equation has oscillatory solutions for real wavenumber and monotonic increasing solutions for imaginary wavenumber. Although the preceding result was obtained only for small radius (37a), it will be extended in the sequel (Subsections 3.2 and 3.3) to all values of the radial distance. Thus the condition specifying wave fields with oscillatory dependence on the radius (39a) is expressed in terms of the dimensionless

4

frequency (38b),

$$\kappa^2 > 0 : \quad \frac{\omega r_0}{c_{00}} > \sqrt{\frac{8}{\gamma} - 1} = \sqrt{\frac{7N-2}{N+2}} = \sqrt{\frac{19}{5}, \frac{33}{7}, 5}\,.$$
$$(39\mathrm{a, b})$$

Using (31b) the condition for radially oscillatory AVE waves is written in terms of the angular velocity,

$$\omega > \frac{c_{00}}{r_0}\sqrt{\frac{8}{\gamma} - 1} = \Omega\sqrt{\frac{\gamma}{2}\left(\frac{8}{\gamma} - 1\right)} = \Omega\sqrt{4 - \frac{\gamma}{2}} = \Omega\sqrt{\frac{7}{2} - \frac{1}{N}} \sqrt{\frac{19}{6}, \frac{33}{10}, \frac{10}{3}}$$
$$(40)$$

Using the sound speed (36a) at the reference radius the oscillatory condition (39b) becomes

$$\frac{\omega r_0}{c_0(r_0)} = \frac{\omega r_0}{c_{00}\sqrt{2}} > \sqrt{\frac{4}{\gamma} - \frac{1}{2}} = \sqrt{\frac{8-\gamma}{2\gamma}} = \sqrt{\frac{7N-2}{2N+4}} = \sqrt{\frac{19}{10}, \frac{33}{14}, \frac{5}{2}}$$
$$(41)$$

Bearing in mind that the vorticity is twice the angular velocity (12b) the oscillatory condition (40) becomes

$$\frac{\omega}{\varpi} = \frac{\omega}{2\Omega} > \sqrt{1 - \frac{\gamma}{8}} = \sqrt{\frac{7}{8} - \frac{1}{4N}} = \sqrt{\frac{7N-2}{8N}} = \sqrt{\frac{19}{24}, \frac{33}{40}, \frac{5}{6}} \equiv \mu\,.$$
$$(42)$$

Of the four forms of the oscillatory condition (39b), (40), (41) and (42) the last is independent of the geometry and may be the most general: a compressible, vortical, non-isentropic flow has perturbations with oscillatory dependence on the radial distance if the frequency is larger than the peak vorticity ϖ multiplied by the factor μ in (42). The spatial growth of perturbations of acoustic-vortical waves [12, 13] is comparable to the temporal growth [9] as an indicator of instability. Thus the oscillatory condition excluding monotonic growth of perturbations could be equivalent to a stability condition for the mean flow. This conjecture can be applied (Figure 1) to combustion stability in a confined space: (i) if the natural frequencies exceed the product $\mu\varpi$ there is (Figure 1a) stability, and only the fundamental frequency needs to be considered $\omega_1 > \mu\varpi$; (ii) if the fundamental frequency and other modes lie below $\mu\varpi$ those modes lead to instability (Figure 1b). The pas-

(a)

(b)
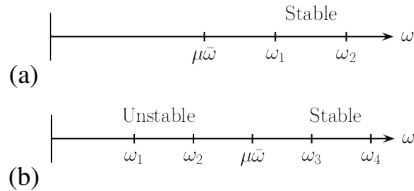
Figure 1: The compressible, vortical, non-isentropic flow is stable if the peak vorticity multiplied by (42) is less than the fundamental frequency (Figure 1a) and unstable otherwise (Figure 1b).

sage from stable to the unstable case could be due to: (i) increasing the vorticity of the mean flow, e.g. to achieve better mixing for 'lean' fuel saving combustion; (ii) in-

creasing the size of the enclosure, so that the natural frequencies reduce, and fall below $\mu\varpi$. The remark (i) agrees with the observation that lean combustion tends to be unstable; the remark (ii) agrees with the observation that larger rocket motors are more prone to large amplitude oscillations. The stability criterion

$$\omega_1 > \mu\varpi_{max}\,, \quad \mu = 0.890, 0.908, 0.913\,, \qquad (43\mathrm{a, b})$$

that the fundamental frequency must be larger than the peak vorticity times the factor (42) can be tested for more complex geometries using numerical codes. It has a simple interpretation: (i) acoustic modes with frequency ω are stable; (ii) vortical modes with vorticity ϖ are unstable; (iii) there is stability if the acoustic modes predominate $\omega > \varpi$; (iv) there is instability if the vortical modes predominate $\varpi > \omega$. The factor (42) involving the adiabatic exponent appears because the vortical modes are incompressible and the acoustic modes are adiabatic and thus the ratio of frequency to vorticity is close to but not exactly unity.

3.2. Regular and logarithmic solutions inside the critical radius

The independent variable is chosen to be the square of the radius divided by the reference radius (44a),

$$s \equiv (r/r_0)^2 = \frac{\Omega^2\gamma r^2}{2c_{00}^2} = \frac{\Omega^2\gamma r^2}{[c_0(r_0)]^2} = \frac{\Omega^2 r^2}{RT_0(r_0)}\,, \quad \tilde{v}_r(r,\omega) = J(s,\kappa)\,,$$
$$(44\mathrm{a, b})$$

that is unity at the radial distance of unit isothermal swirl Mach number. The acoustic-vortical-entropy wave equation (32) becomes

$$s^2(1+s)J'' + s(1+2s)J' + [(\kappa^2 s - 1)/4]J = 0\,, \quad (45)$$

that involves as parameter only the radial wavenumber (38b), that includes all compressibility, vorticity and non-isentropic effects. The zero or infinite values of the coefficient of the highest order derivative (46a) determine the singularities of the differential equation (45), namely (46b),

$$s^2(1+s) = 0, \infty : \qquad s = 0, \infty, -1, \quad r = 0, \infty, \pm ir_0\,.$$
$$(46\mathrm{a-c})$$

From the location (Figure 2) of the singularities (46c) it follows that: (i) the singularities at the origin $r = 0$ and infinity $r = \infty$ lead to a pair of solutions respectively in ascending $W_\pm$ and descending $W^\pm$ powers of the radius; (ii) the singularities at $|r| = r_0$ imply that the ascending series solution converges for $|r| < r_0$ and the descending series solution converges for $|r| > r_0$; (iii) even if either or both series do not converge at the circle of convergence, a pair of solutions $W_{1,2}$ around the critical radius overlaps with the first two and allows

5

their matching (Figure 2). In this way the exact solution of the AVE wave equation can be obtained for all radial distances, as shown next (Subsections 3.2 and 3.3 and Section 4).
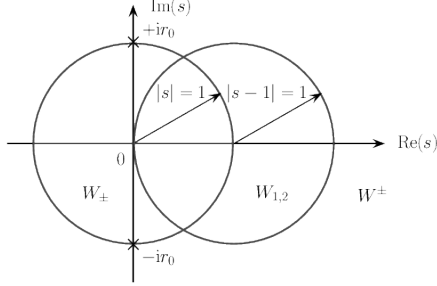
Figure 2: The AVE wave equation (32) rewritten (45) in terms of the variables (44a,b) has singularities at (46a–c) implying that: (i) the pair of solutions $W_\pm$ around the singularity at the origin are series of ascending powers of the radius that converge inside the critical layer $0 \leq r < r_0$; (ii) the pair of solutions $W^\pm$ around the singularity at infinity are series of descending powers of the radius that converge outside the critical layer $r_0 < r \leq \infty$; (iii) the two pairs of solutions (i) and (ii) are matched by a third pair $W_{1,2}$ around the critical radius that are power series of $(r/r_0)^2 - 1$ with region of convergence overlapping with those of $W_\pm$ and $W^\pm$.

The origin is a regular singularity [14] of the differential equation (45), and thus at least one solution exists as a Frobenius-Fuchs series of ascending powers of the radius,

$$|s| < 1 : \qquad J_\sigma(s, \kappa) = \sum_{n=0}^{\infty} a_n(\sigma) s^{n+\sigma}, \qquad (47a, b)$$

with index σ and coefficients to be determined. Substituting (47b) in (45) leads to

$$\left[(n+\sigma)^2 - 1/4\right] a_n(\sigma) = - \left[(n+\sigma-1)(n+\sigma) + \kappa^2/4\right] a_{n-1}(\sigma). \qquad (48)$$

Setting (49a) leads to the indicial equation (49b) with roots (49c),

$$n = 0 : \qquad (\sigma^2 - 1/4)a_0(\sigma) = 0 \Rightarrow \sigma = \pm 1/2. \qquad (49a - c)$$

The solution corresponding to the upper root (50a) has recurrence formula (48) for the coefficients (50b),

$$\sigma = 1/2 : \quad a_n(1/2) = -\frac{n^2 + (\kappa^2 - 1)/4}{n(n+1)} a_{n-1}(1/2). \qquad (50a, b)$$

This double recurrence formula specifies explicitly the coefficients (51b),

$$a_0(1/2) = 1 : a_n(1/2) = \frac{(-)^n}{n!(n+1)!} \prod_{m=1}^{n} \left[m^2 + (\kappa^2 - 1)/4\right] \equiv a_n^+, \qquad (51a, b)$$

where the first coefficient may be set to unity (51a) be-cause the solution is valid to within a multiplying constant. Substitution of (50a;51b) in (47a,b;44a,b) specifies the radial velocity perturbation,

$$r < r_0 : \qquad W_+(r, \kappa) = \sum_{n=0}^{\infty} a_n^+ (r/r_0)^{2n+1} = J_{1/2}(s, \kappa), \qquad (52a, b)$$

that vanishes at the origin like $O(r)$, in agreement with the Bessel function $J_1(\kappa r)$ that is the solution of (37b) for small radius.

The indexes (49c) differ by an integer (53a) and thus the second solution [15] is given by (53b),

$$\sigma_+ - \sigma_- = 1 : \quad W_-(r, \kappa) = Y_{-1/2}(s, \kappa) = \lim_{\sigma \to -1/2} \frac{\partial}{\partial \sigma} \left[(\sigma + 1/2) J_\sigma(s, \kappa)\right]. \qquad (53a, b)$$

The solution (53b) is a function of the second kind,

$$Y_-(s, \kappa) = \log s \sum_{n=0}^{\infty} a_n^+ s^{n-1/2} + \sum_{n=0}^{\infty} a_n^- s^{n-1/2}, \quad (54)$$

that consists of a logarithmic singularity multiplied by a function of the first kind plus a complementary function that has a power type singularity $s^{-1/2}$. The notation (J, Y) is used for the solutions regular (47b) and singular (54) at the origin, as for Bessel and Neumann functions respectively, of which they are an extension for (37a) to $r < r_0$. The coefficients a_n^- follow by substitution in (53b) of (47b) with the recurrence formula (48) leading to (55),

$$n \geq 1 : a_n^- = a_n^+ \left[\psi(n+1+\nu/2) + \psi(n+1-\nu/2) - \psi(n+2) - \psi(n)\right], \qquad (55a, b)$$

where appears the ψ function [16, 4] and (56b),

$$\nu \equiv \sqrt{1 - \kappa^2}; \quad a_0^- = -(\kappa^2 - 1)(\kappa^2 - 3)/16, \quad (56a, b)$$

The exception to (55a,b) is the coefficient (56b) as can be confirmed in Subsection 4.1. The solution of the second kind,

$$r < r_0 : \qquad W_-(r, \kappa) = 2\log(r/r_0) \sum_{n=0}^{\infty} a_n^+ (r/r_0)^{2n+1} + \sum_{n=0}^{\infty} a_n^- (r/r_0)^{2n-1}, \qquad (57a, b)$$

consists of two terms: (i) the logarithmic singularity in the first term on the r.h.s. of (57) is dominated by the factor r/r_0 as $r \to 0$, so this term vanishes at the origin; (ii) the second term on the r.h.s. of (57) has a singularity r_0/r at the origin with coefficient (56b). The general integral is a linear combination of the two solutions:

$$0 \leq r < r_0 : \tilde{v}_r(r, \omega) = C_+ W_+(r, \kappa) + C_- W_-(r, \kappa), \qquad (58a, b)$$

where $C_\pm$ are arbitrary constants.

3.3. Asymptotic series outside the critical radius

The solution (58b) is valid inside the reference radius (58a), and the solution valid outside is obtained using

6

the inverse (59a) of the variable (44a),

$$\zeta = \frac{1}{s} = (r_0/r)^2 \,, \quad \tilde{v}_r(r, \omega) = J(s, \kappa) = H(\zeta, \kappa) \,,$$
$$(59\mathrm{a,b})$$

leading from (45) to the differential equation

$$\zeta^2(\zeta + 1)H'' + \zeta^2 H' + [(\kappa^2 - \zeta)/4]H = 0 \,. \quad (60)$$

The point at infinity $r = \infty$ corresponds to the origin $\zeta = 0$ of (59a), that is a regular singularity of the differential equation (60) implying the existence of a Frobenius-Fuchs series solution,

$$\zeta < 1 : \quad H_\vartheta(\zeta, \kappa) = \sum_{n=0}^{\infty} b_n(\vartheta)\zeta^{n+\vartheta} \,, \quad (61\mathrm{a,b})$$

that corresponds to a descending power series of the radius,

$$r > r_0 : \quad \tilde{v}_r(r, \omega) = \sum_{n=0}^{\infty} b_n(\vartheta)(r_0/r)^{2n+2\vartheta} \,. \quad (62\mathrm{a,b})$$

Substitution of (61b) in (60) leads to the recurrence formula for the coefficients:

$$\left[(n+\vartheta)(n+\vartheta-1) + \kappa^2/4\right]b_n(\vartheta) = -\left[(n+\vartheta-1)^2 - 1/4\right]b_{n-1}(\vartheta).$$
$$(63)$$

Setting (64a) leads to the indicial equation (64b),

$$n = 0 : \quad (\vartheta^2 - \vartheta + \kappa^2/4)b_0(\vartheta) = 0 \Rightarrow 2\vartheta_\pm = 1 \pm \sqrt{1 - \kappa^2} = 1 \pm \nu \,,$$
$$(64\mathrm{a-c})$$

that has roots (64c) where appears (56a). The corresponding recurrence formula for the coefficients is

$$b_n(\vartheta_\pm) = -\frac{(n \pm \nu/2 - 1/2)^2 - 1/4}{(n \pm \nu/2 + 1/2)(n \pm \nu/2 - 1/2) + \kappa^2/4}b_{n-1}(\vartheta_\pm).$$
$$(65)$$

The double recurrence formula (65) allows explicit calculation of the coefficients,

$$b_0(\vartheta_\pm) = 1 : b_n(\vartheta_\pm) = (-)^n \prod_{m=1}^{n} \frac{(2m \pm \nu)(2m \pm \nu - 2)}{(2m \pm \nu)^2 - 1 + \kappa^2} \,.$$
$$(66\mathrm{a,b})$$

The corresponding solutions (62a,b) are

$$r > r_0 : W^\pm(r, \kappa) = \sum_{n=0}^{\infty} b_n^\pm(r_0/r)^{2n+1\pm\nu} = H_{\vartheta_\pm}(\zeta, \kappa) \,,$$
$$(67\mathrm{a,b})$$

are linearly independent for $\nu \neq 0$ and will be checked in Subsection 4.2. The general integral is their linear combination,

$$r > r_0 : \tilde{v}_r(r, \omega) = C^+ W^+(r, \kappa) + C^- W^-(r, \kappa) \,,$$
$$(68\mathrm{a,b})$$

involving the arbitrary constants $C^\pm$. If $\nu > 1$, that is for $\kappa^2 < 0$ or imaginary κ in (56a), the solution W^- diverges (67b) as $r \to \infty$, and must be suppressed setting $C^- = 0$, leaving only the solution W^+. The latter would also diverge as $r \to \infty$ if $\mathrm{Re}(\nu) < -1$, but this is not possible since ν in (56a) is either imaginary for $\kappa^2 > 1$ or $\nu > -1$ for $\kappa^2 \leq 1$. Thus the solution W^+ is

always bounded at infinity. The two solutions (67b) are oscillatory (69b) for $\kappa^2 > 1$ or imaginary ν,

$$\nu = \mathrm{i}|\nu| : \quad (r_0/r)^{1\pm\nu} = (r_0/r)^{1\pm\mathrm{i}|\nu|} = (r_0/r)\exp\left[\pm\mathrm{i}|\nu|\log(r_0/r)\right] \,,$$
$$(69\mathrm{a,b})$$

and vanish at infinity. For $0 < \kappa^2 < 1$ then $|\nu_\pm| < 1$ in (56a) and both solutions (67a,b) converge. In conclusion: (i) for imaginary radial wavenumber $\kappa^2 < 0$, that is the opposite of (39a), there is monotonic radial growth inside the critical radius, and outside the critical radius W^- in (67b) diverges as $r \to \infty$ since $|\nu| > 1$ in (56a); (ii) for $\kappa^2 > 1$ that satisfies (39a) there is oscillation inside the critical radius and since ν is imaginary in (56a) the solutions outside the critical radius (69a,b) are oscillatory and decaying; (iii) for $0 < \kappa^2 < 1$ the radial oscillation inside the critical radius remains (39a) and since $|\nu| < 1$ in (56a) the solutions (67a,b) outside the critical radius are monotonic and decaying. The oscillatory condition $\kappa^2 > 0$ in (39a) corresponds to (39b,40,41,42) and the monotonic condition $\kappa^2 < 0$ to the reverse. The condition (70a) of oscillatory waves at infinity (69a,b) corresponds (38b,c) to (70b),

$$\kappa^2 > 1 : \quad \bar{\omega} = \frac{\omega r_0}{c_{00}} > \sqrt{\frac{8}{\gamma}} = \sqrt{\frac{8N}{N+2}} = \sqrt{\frac{24}{5}, \frac{40}{7}}, 6 \,.$$
$$(70\mathrm{a,b})$$

4. MATCHING OF INNER AND OUTER SOLUTIONS ACROSS THE CRITICAL LAYER

4.1. Transformation to a Gaussian hypergeometric differential equation

The differential equation (45) was solved using directly the Frobenius-Fuchs method since this is the quickest way to obtain the acoustic-vortical-entropy wave field (52a,b;51a,b). The solutions can be obtained alternatively in terms of Gaussian hypergeometric functions by means of changes of dependent and independent variables indicated next. The change of dependent variable (71a) in (45) leads to (71b),

$$J(s) = s^\alpha K(s) :$$
$$(71\mathrm{a})$$
$$s^2(1+s)K'' + s[1+2\alpha+2(1+\alpha)s]K' + [(\alpha^2+\alpha+\kappa^2/4)s+\alpha^2-1/4]K = 0 \,,$$
$$(71\mathrm{b})$$

where the constant α may be chosen at will. Choosing (72a) allows (71b) to be divided through s, depressing the degree of the coefficients from three in (71b) to two in (72b),

$$\alpha = \frac{1}{2} : \quad s(1+s)K'' + (2+3s)K' + [(\kappa^2+3)/4]K = 0 \,.$$
$$(72\mathrm{a,b})$$

A further change of independent variable (73a,b) leads to (73c),

$$u = -s \,, K(s) = Q(u) : \quad u(1-u)Q'' + (2-3u)Q' - [(\kappa^2+3)/4]Q = 0 \,.$$
$$(73\mathrm{a-c})$$

The latter is a Gaussian hypergeometric differential equation [17],

$$u(1-u)Q'' + [C - (A+B+1)u]Q' - ABQ = 0 \,, \quad (74)$$

7

with parameters satisfying (75a-c),

$$C = 2\,,\ A{+}B = 2\,,\ AB = \frac{\kappa^2 + 3}{4}\ :\quad A, B = 1{\pm}\frac{1}{2}\sqrt{1 - \kappa^2} = 1{\pm}\frac{\nu}{2}\,,$$
$$(75a - d)$$

and implying (75d).

Since $C = 2$, there is only one solution without logarithmic singularity at $u = 0$, namely the Gaussian hypergeometric function of the first kind,

$$Q_+(u) = F(A, B; C; u) = 1 + \sum_{n=1}^{\infty} \frac{u^n}{n!} \prod_{m=1}^{n} \frac{(A + m - 1)(B + m - 1)}{(C + m - 1)}$$
$$(76)$$

where was used the hypergeometric series. Substitution of (75a-c,73a,72a,71a,44a) leads to

$$\begin{aligned}
\tilde{v}_r^1 &= \frac{r}{r_0} F\left(A, B; 2; -\frac{r^2}{r_0^2}\right) \\
&= \frac{r}{r_0}\left[1 + \sum_{n=1}^{\infty} \frac{(r/r_0)^{2n}}{n!(n+1)!}(-)^n \prod_{m=0}^{n}\left(m^2 + \frac{\kappa^2 - 1}{4}\right)\right]
\end{aligned}$$

that coincides with (52b,51b).

4.2. Power and logarithmic singularities of the functions of the first and second kind

The solution with logarithmic singularity at the origin is a function of the second kind [17],

$$Q_-(u) = G(A, B; 2; u) = F(A, B; 2; u)\log u + H(A, B; 2; u)\,,$$
$$(78)$$

with the complementary function $H(A, B; 2; u)$, where the ψ function [16, 4] is the logarithmic derivative of the Gamma function. In the case of acoustic-vortical-entropy waves, besides the first solution (77), the second solution is

$$\tilde{v}_r^2(r, \kappa) = 2\log(r/r_0)W_+(r, \kappa) + W_*(r, \kappa) \equiv W_-(r, \kappa)\,,\ (79)$$

including: (i) the regular solution (77) multiplied by a logarithmic singularity; (ii) plus the complementary function that has an algebraic singularity,

$$W_*(r, \kappa) = -\frac{(\kappa^2 - 1)(\kappa^2 + 3)}{16}\frac{r_0}{r}$$
$$+ \sum_{n=1}^{\infty} \frac{(-)^n}{n!}\frac{(r/r_0)^{2n}}{(n+1)!}\left[\prod_{m=1}^{n}\left(m^2 + \frac{\kappa^2 - 1}{4}\right)\right]$$
$$\{\psi(n + 1 + \nu/2) + \psi(n + 1 - \nu/2) - \psi(n + 2) - \psi(n)\}\ (80)$$

Thus the solution finite on axis consists only of the function of the first kind (77) and holds $|r| < r_0$ inside the critical radius. The solution (78) in terms of the function of the second kind can be written

$$W_-(r, \kappa) = 2\log(r/r_0)W_+(r, \kappa) + W_*(r, \kappa)\,,\quad (81)$$

that coincides with (57b) because it consists of the sum of: (i) the function of the first kind (77)≡(52b;51b) multiplied by a logarithmic singularity; (ii) the function of the second kind (80) that coincides with the second term of the r.h.s. of (57b) with coefficient (55b); (iii) the algebraic term r/r_0 in the function of the second kind, corresponding to the first term of the r.h.s. of (80) has

coefficients

$$a_0^- = A(A - 1)B(B - 1) = \frac{\kappa^2 + 3}{4}\frac{\kappa^2 - 1}{4}\,,\quad (82)$$

in agreement with (56b). This completes the pair of solutions of the AVE wave equation inside the critical radius (58a,b).

The wave fields outside the critical radius correspond to the solutions of the hypergeometric equation around the point at infinity [18].

4.3. AVE wave field at and around the critical layer

The parameters (75a,b) of the hypergeometric function satisfy $C - A - B = 0$, implying [19, 4] that: (i) there is conditional convergence on the boundary of convergence $|s| = 1$ or $|r| = r_0$ excluding the point $\bar{s} = W_+(\bar{r}, \kappa) = r^2/r_0^2$ or $r = \pm ir_0$; (ii) at this point there is divergence. This shows that the radial velocity perturbation spectrum is finite at the critical radius, as it will be confirmed subsequently (91a,b). This can be confirmed by obtaining the solution of the acoustic-vortical-entropy wave equation around the critical radius. The Gaussian hypergeometric differential equation (74) transforms into itself with different parameters by the changes of independent variable in the Schwartz group,

$$u,\ 1 - u,\ \frac{1}{u},\ 1 - \frac{1}{u},\ \frac{u - 1}{u},\ \frac{u}{u - 1}\,,\quad (83)$$

that interchange between themselves the three regular singularities: $u = 0, 1, \infty$. Since $s > 0$ in (44a) and $u < 0$ in (73a), the variable (84a) does not exceed unity,

$$\xi \equiv \frac{u}{u - 1} = \frac{s}{s + 1} = \frac{r^2}{r^2 + r_0^2} < 1\,,\quad |r - r_0| < r_0\,,$$
$$(84a, b)$$

and the corresponding series solution converges for (84b) that is from the origin to twice the critical radius. The solutions of the Gaussian hypergeometric differential equation in terms of the variable (84a) are [17, 18]

$$Q_1(u) = (1 - u)^{-A}F(A, C - B; C; u/(u - 1))\,,\quad (85a)$$

$$Q_2(u) = u^{1-C}(1 - u)^{C-A-1}F(A - C + 1, 1 - B; 2 - C; u/(u - 1))\quad (85b)$$

Substituting (75a,d), (84a) and (73a,b; 72a; 71a; 44a,b) leads to

$$W_1(r; \kappa) = (1 + r^2/r_0^2)^{-1-\nu/2}F(1 + \nu/2, 1 + \nu/2; 2; r^2/(r_0^2 + r^2))\quad (86a)$$

$$W_2(r; \kappa) = -(r_0^2/r^2)(1 + r^2/r_0^2)^{-\nu/2}F(\nu/2, \nu/2; 0; r^2/(r_0^2 + r^2))\quad (86b)$$

The radial velocity perturbation spectrum is a linear combination of (86a,b),

$$0 < r < 2r_0\ :\quad W(r; \kappa) = C_1 W_1(r; \kappa) + C_2 W_2(r; \kappa)\,,$$
$$(87a, b)$$

and is valid (84b) from the axis to twice the critical radius (87a). The value at the critical radius $r = r_0$ corresponds to $\xi = 1/2$ and is finite. Since the AVE wave

field has been determined exactly for all values of the radius, it is possible to consider AVE wavemodes in cylindrical or annular ducts for any values of the radii. For example, the wave field up to two critical radii (87a) is given by (87b) where (86b) is singular on axis and must be excluded for a cylindrical duct setting (88a) and leading to (88b),

$$C_2 = 0 : \quad W(r;\kappa) = C_1(1+r^2/r_0^2)^{-1-\nu/2}F(1+\nu/2, 1+\nu/2; 2; r^2/(r_0^2+r^2)) .$$
$$(88a, b)$$

The application of rigid or impedance wall boundary conditions then specifies the eigenvalues and eigenfunctions of AVE modes (Section 5).

5. VELOCITY, PRESSURE, DENSITY, ENTROPY AND TEMEPRATURE PERTURBATIONS

5.1. Divergence of the inner and outer wave fields at the critical radius

The exact inner (outer) solutions of the AVE wave equations converge respectively inside (outside) the critical radius thus specifying the acoustic (vortical) modes; the critical layer, where mode conversion occurs, corresponds to the boundary of convergence of both the inner and outer series solutions. The convergence on the boundary of convergence [4] is specified by the ratio of successive coefficients (51b) [(66b)] in (89) [(90)],

$$\frac{a_{n+1}^+}{a_n^+} = -\frac{n^2 + 2n + (\kappa^2 + 3)/4}{n^2 + 3n + 2} , \qquad (89)$$

$$\frac{b_{n+1}^\pm}{b_n^\pm} = -\frac{4n^2 + 4n(1 \pm \nu) + \nu^2 \pm 2\nu}{4n^2 + 4n(2 \pm \nu) + 4(1 \pm \nu)} . \qquad (90)$$

The limit as $n \to \infty$ is

$$\left| \frac{a_{n+1}^+}{a_n^+} \right| = 1 - \frac{1}{n} + O\left(\frac{1}{n^2}\right) = \left| \frac{b_{n+1}^\pm}{b_n^\pm} \right| . \qquad (91a, b)$$

The combined convergence test [20, 4, p.494] on the boundary of convergence applies to a ratio of terms,

$$\left| \frac{u_{n+1}}{u_n} \right| = 1 - \frac{g}{n} + O\left(\frac{1}{n^2}\right) , \qquad (92)$$

and is specified by the value of g. Thus $g = 1$ implying that: (i) both series diverge for $-(r/r_0)^2 = 1$, that is at the singular points $r = \pm ir_0$; (ii) at all other points on the circle of $|-(r/r_0)^2| = 1$ or $|r| = r_0$, the series are conditionally convergent, that is: (ii-1) converge if the order of the terms is not deranged; (ii-2) the series of moduli diverges. Since r is real and positive, the only point on the circle of convergence of physical interest is the critical radius $r = r_0$, where both the inner and outer series for radial velocity perturbation spectrum converge conditionally and can be matched

directly. However, the direct matching would also require the pressure perturbation (33e) to be continuous; since it has been shown that $\tilde{v}_r$ is continuous across the critical radius for the direct matching to be possible, $\tilde{v}_r'$ must also be continuous. From (52b) [(67b)] follows the derivative of the radial velocity perturbation for acoustic (vortical) modes inside (outside) the critical radius (93) [(94)] .

$$W_+'(r,\kappa) = \frac{1}{r_0} \sum_{n=0}^{\infty} (2n + 1)a_n^+(r/r_0)^{2n} , \qquad (93)$$

$$[W^\pm(r,\kappa)]' = \frac{1}{r_0} \sum_{n=0}^{\infty} (2n + 1/2 \pm \nu/2)b_n^\pm(r/r_0)^{2n \pm \nu} . \qquad (94)$$

As $n \to \infty$ both a_n^+ $(b_n^\pm) \to 1$ tend to unity in (51b) [(66a,b)] and thus the coefficients in (93) [(94)] are $O(n)$, implying divergence on the critical radius $r = r_0$. Thus the pressure perturbation is singular at the critical radius, both for the acoustic and vortical modes, and matching is not possible using directly the inner and outer solutions. The matching can always be performed using the middle solution valid around the critical layer, where the AVE wave field is finite.

5.2. Waves inside or outside a cylinder or in a cylindrical annulus

It has been shown that there are acoustic-vortical-entropy waves finite over the whole range of radial distances leading to (Figure 3) six possibilities: (i–ii) the interior (exterior) of a cylinder inside (outside) the critical radius (Figure 3a) that is using the inner (outer) solution in a cylinder (cylindrical cavity); (iii–iv) a cylindrical annulus either inside or outside the critical radius (Figure 3b); (v–vi) a cylinder (Figure 3c) or cylindrical annulus (Figure 3d) containing the critical layer, using the middle solution alone if the outer radius is less than twice the critical radius, or otherwise matching to the outer solution. The oscillatory or monotonic radial dependence of the wave fields is specified by the inner and outer solutions as indicated in the Table 1. Focusing on case VI and the simplest boundary condition of a rigid wall at $r = a$ with zero radial velocity (95a),

$$\tilde{v}_r(a, \omega) = 0 : \quad F(1+\nu/2, 1+\nu/2; 2; a^2/(r_0^2+a^2)) = 0 , \qquad (95a, b)$$

leads to (95b). The Gaussian hypergeometric function in (95b) can be calculated most efficiently summing the series (96a) with the recurrence formula for the successive terms (96c),

$$G(\xi; \nu) \equiv F(1 + \nu/2, 1 + \nu/2; 2; \xi) = 1 + \sum_{n=1}^{\infty} f_n(\xi) , \qquad (96a)$$

9
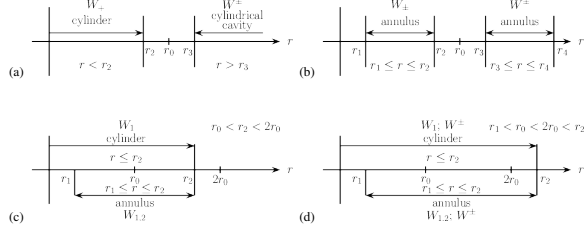
Figure 3: AVE wave equation solution in (a) a cylinder (cylindrical cavity) not containing the critical layer, (b) annulus inside (outside) the critical layer, (c) cylinder (cylindrical annulus) with (outer) radius less than twice the critical layer radius; (d) cylinder (annulus) with (outer) radius larger than twice the critical radius.

Case	Radius	Solution	Bounded	
			Oscillatory	Monotonic
I cylindrical cavity	$r_0 < r_3 \leq r < \infty$	$C^+ W^+(r)$	-	$\kappa^2 < 0$
		$C^+ W^+(r) + C^- W^-(r)$	$\kappa^2 > 1$	-
		$C^+ W^+(r) + C^- W^-(r)$	-	$0 < \kappa^2 < 1$
II vortical annulus	$r_0 < r_3 \leq r \leq r_4 < \infty$	$C^+ W^+(r) + C^- W^-(r)$	$\kappa^2 > 1$	$\kappa^2 < 1$
III acoustic annulus	$0 < r_1 \leq r \leq r_2 < r_0$	$C_+ W_+(r) + C_- W_-(r)$	$\kappa^2 > 0$	$\kappa^2 < 0$
IV cylinder	$0 \leq r \leq r_4 < r_0$	$C_+ W_+(r)$	$\kappa^2 > 0$	$\kappa^2 < 0$
V cylindrical annulus	$0 \leq r_1 \leq r \leq r_2$ $r_1 < r_0 < r_2$	$C_1 W_1(r) + C_2 W_2(r)$	$\kappa^2 > 0$	$\kappa^2 < 0$
VI cylinder	$0 \leq r \leq r_2$ $r_0 < r_2 < 2r_0$	$C_1 W_1(r)$	$\kappa^2 > 0$	$\kappa^2 < 0$

Note: there is no case of unbounded oscillation.

Table 1: Exact solutions of the acoustic-vortical-entropy wave equation indicating the six cases of the stability of the mean flow in the four configurations in the Figure 3.

$$f_0(\xi) = 1, \quad f_{n+1}(\xi) = f_n(\xi) \frac{(n+1+\nu/2)^2}{(n+1)(n+2)} \xi.$$
(96b, c)

The eigenvalues for the radial wavenumber are the roots of (97),

$$0 = G\left(\frac{1}{1+(r_0/a)^2}; \sqrt{1-\kappa^2}\right) = G_0 \prod_{l=1}^{\infty}(\kappa - \kappa_l), \quad (97)$$

where G_0 is a constant. To each eigenvalue corresponds (86a;96a) an eigenfunction,

$$\bar{v}_l(r/r_0) = (1+r^2/r_0^2)^{-1-\nu/2} G\left(\frac{1}{1+(r_0/r)^2}; \sqrt{1-\kappa^2}\right).$$
(98)

The eigenvalues κ_l for the radial wavenumber specify the eigenfrequency $\bar{\omega}_l$ by (38b) with the adiabatic exponent $\gamma = 1.4$ for a diatomic perfect gas.

5.3. Eigenvalues for the wavenumber and frequency and eigenfunctions for six wave variables

The AVE waves are considered inside a cylinder with radius (99a) for the fours cases (99b),

$$0 \leq r \leq a : \quad a/r_0 = 0.4, 0.8, 1.2, 1.6, \quad (99a, b)$$

of which the first (last) two do not (do) contain the critical layer. For each cylinder the roots of (95b) specify the first six eigenvalues κ_l of the radial wavenumber ordered by non-decreasing modulus in the Table 2; the corresponding dimensionless natural frequencies $\bar{\omega}_l$ follow from (38b) and appear in the Table 3. To each pair of dimensionless eigenvalues $(\kappa_l, \bar{\omega}_l)$ correspond six dimensionless eigenfunctions for distinct wave variables, namely the dimensionless: (i) radial velocity (98) with magnitude unity at the origin,

$$D_l \equiv G\left(1; \sqrt{1-\kappa_l^2}\right) : \bar{v}_l(r/r_0) = \frac{\tilde{v}_r(r, \omega)}{D_l},$$
(100a, b)

that is plotted in the Figure 4; (ii) azimuthal (33a) velocity (101),

$$\bar{w}_l(r/r_0) \equiv \frac{c_{00}}{\Omega r_0} \frac{\tilde{v}_\varphi(r, \omega)}{D_l} = -i\frac{2}{\bar{\omega}_l} \bar{v}_l(r/r_0), \quad (101)$$

that is plotted in the Figure 5; (iii) the mass (33b) density (102),

$$\bar{\rho}_l(r/r_0) \equiv \frac{c_{00}}{D_l} \frac{\tilde{\rho}}{\rho_0} = -\frac{i}{\bar{\omega}_l}[\bar{v}_l' + (r_0/r)\bar{v}_l], \quad (102)$$

that is plotted in the Figure 6; (iv) the (33d) entropy (103),

$$\bar{s}_l(r/r_0) \equiv \frac{c_{00}}{D_l} \frac{\tilde{s}(r, \omega)}{C_V} = -\frac{2i}{\bar{\omega}_l} \frac{1}{r/r_0 + r_0/r} \bar{v}_l, \quad (103)$$

10

that is plotted in the Figure 7; (v) the (33e) pressure (104),

$$\bar{p}_l(r/r_0) = -\frac{\mathrm{i}}{\bar{\omega}_l} \left\{ \left[(1 + 2/\gamma)\, r/r_0 + r_0/r \right] \bar{v}_l + \left(1 + r^2/r_0^2 \right) \bar{v}_l' \right\},$$

(104)

that is plotted in the Figure 8.

The temperature perturbation (33c) follows (106) from those of the density (102) and pressure (104),

$$\bar{T}_l(r/r_0) \equiv \frac{c_{00}}{D_l} \frac{\tilde{T}(r,\omega)}{T_0} = \qquad (105)$$

$$= \frac{r_0^2}{2r^2} [M(r)]^2 \bar{p}_l(r/r_0) - \bar{\rho}_l(r/r_0),$$

that is plotted in the Figure 9. It involves the isothermal swirl Mach number,

$$\gamma \frac{c_{00}^2}{[c_0(r)]^2} = \frac{r_0^2}{2r^2} \frac{\gamma^2 \Omega^2 r^2}{[c_0(r)]^2} = \frac{r_0^2}{2r^2} [M(r)]^2, \qquad (106)$$

where were used (31a,b). In (102) and (104) appear the derivative with regard to its argument (107) of the radial velocity (100),

$$\bar{v}_r'(r/r_0) \equiv \frac{\mathrm{d}[\bar{v}_r(r(r_0)]}{\mathrm{d}(r/r_0)} =$$

$$= -\frac{2+\nu}{D_l} \frac{r}{r_0} \left(1 + r^2/r_0^2 \right)^{-2-\nu/2} F\left(1+\nu/2, 1+\nu/2; 2; \xi \right)$$

$$+ \frac{(1+\nu/2)^2}{D_l} \frac{r_0^3 r}{(r_0^2 + r^2)^2} F\left(2+\nu/2, 2+\nu/2; 3; \xi \right), \qquad (107)$$

where was used (108a) the derivative (108b) of the Gaussian hypergeometric function in (96a),

$$\frac{\mathrm{d}\xi}{\mathrm{d}(r/r_0)} = \frac{2r_0^3 r}{(r_0^2 + r^2)^2},$$

(108a)

$$\frac{\mathrm{d}}{\mathrm{d}\xi} \left[F\left(1+\nu/2, 1+\nu/2; 2; \xi \right) \right] = \frac{(1+\nu/2)^2}{2} F\left(2+\nu/2, 2+\nu/2; 3; \xi \right).$$

(108b)

The Gaussian hypergeometric series in (108b) is calculated as (96a–c) replacing ν by $1 + \nu$.

6. WAVEFORMS FOR THE FUNDAMENTAL AND STABLE AND UNSTABLE HARMONICS

The radius of the cylindrical duct is taken as the largest $a/r_0 = 1.6$ of the values in (99b) to show the variation of the AVE wave variables across the critical layer. The modulus and phase of the six corresponding eigenfunctions are plotted versus radial distance in the Figure 4 for the radial velocity (100b), in the Figure 5 for the azimuthal velocity (101), in the Figure 6 for the mass density (102), in the Figure 7 for the entropy (103), in the Figure 8 for the pressure (104) and in the Figure 9 for the temperature (106); for all six wave variables are considered as dimensionless perturbation spectra using the amplitude D_l of the radial velocity perturbation spectrum at the axis. For this reason, all

waveforms or eigenfunctions start with the value unity on the axis in the Figure 4.

The dimensionless radial velocity perturbation spectra in the Figure 4 all start with the value unity on axis due to the normalization and all finish with zero at the rigid wall at $r = 1.6r_0 = a$. The fundamental mode $\bar{v}_1$ has no other zero, and decays smoothly from the axis to the wall. As typical of eigenvalue problems, the harmonics $\bar{v}_n$ of order $n = 2, 3, 4$ have $n - 1$ zeros of the amplitude (Figure 4 top) between the axis and the wall, corresponding to phase jumps of π (Figure 4 bottom). The fifth and sixth harmonics $n = 5, 6$ have complex radial wavenumbers in the Table 2, leading to radially decaying or divergent modes; the divergent modes signal instabilities of the mean as can be seen from the increasing amplitudes of $\bar{v}_5^+$ and $\bar{v}_6^+$ (Figure 4 top). The dimensionless azimuthal velocity perturbation spectrum (Figure 5) also vanishes at the rigid wall for the fundamental $\bar{w}_1$ and next three harmonics $\bar{w}_2$, $\bar{w}_3$, $\bar{w}_4$ (Figure 5 top), again with phase jumps of π at the zeros of the amplitude or nodes (Figure 5 bottom). The fifth and sixth harmonics $\bar{w}_5^+$, $\bar{w}_6^+$ are unstable modes both for the radial (Figure 4 top) and azimuthal (Figure 5 top) velocity perturbations spectra. The amplitude of the dimensionless azimuthal velocity perturbation spectrum on axis (Figure 5 top) decreases from the fundamental to the higher harmonics.

The perturbation spectrum of the mass density (Figure 6) leads to eigenfunctions that are quite different from those of the radial (Figure 4) and azimuthal (Figure 5) velocity perturbation spectra. The mass density perturbation spectra do not vanish at the rigid wall (Figure 6 top) although their magnitude decreases from the fundamental $\bar{\rho}_1$ to the next three stable harmonics $\bar{\rho}_2$, $\bar{\rho}_3$, $\bar{\rho}_4$. The fundamental $\bar{\rho}_1$ almost vanishes at $r = 0.48r_0$ leading to rapid phase change of π (Figure 6 bottom). Whereas the fundamental $\bar{\rho}_1$ has one dip, the next three $n = 2, 3, 4$ harmonics $\bar{\rho}_n$ have n dips, and the fifth and sixth harmonics $\bar{\rho}_5^+$, $\bar{\rho}_6^+$ are unstable as before. The dimensionless entropy perturbation spectrum (Figure 7) vanishes on axis for all harmonics, including the unstable ones $\bar{s}_5^+$, $\bar{s}_6^+$, and vanishes also at the rigid wall for the fundamental $\bar{s}_1$ and the first three stable harmonics $\bar{s}_2$, $\bar{s}_3$, $\bar{s}_4$. The fundamental $\bar{s}_1$ has no zeros and exhibits a single peak at $r = 0.5r_0$ far from the critical layer. The first three harmonics $\bar{s}_n$ with $n = 2, 3, 4$ have n peaks and $n - 1$ nodes. The peaks are lower when: (i) passing from the fundamental $n = 1$ to the harmonics $n = 2, 3, 4$; (ii) for a given harmonic n, the successive n peaks become lower farther from the axis.

The dimensionless pressure perturbation spectra (Figure 8) are broadly similar to those of the mass den-

sity (Figure 6), with similar features, such as a non-zero pressure at the rigid wall with amplitude decreasing from the fundamental $\bar{p}_1$ to the first three stable harmonics $\bar{p}_2$, $\bar{p}_3$, $\bar{p}_4$. The fifth and sixth harmonics $\bar{p}_5^+$, $\bar{p}_6^+$ remain unstable. The fundamental $\bar{p}_1$ has one dip of the amplitude (Figure 8 top) broader than for the mass density (Figure 6 top) and approximately at the same location $r = 0.48r_0$. The next three stable harmonics $\bar{p}_n$ with $n = 2, 3, 4$ have n dips and n peaks (Figure 8 top) with phase jumps (Figure 8 bottom) indicating that the dips are actually zeros or nodes. The dimensionless temperature perturbation spectra (Figure 9) have eigenfunctions broadly similar to the entropy (Figure 7), with: (i) zero on axis for all modes, stable $\bar{T}_1$, $\bar{T}_2$, $\bar{T}_3$, $\bar{T}_4$ or unstable $\bar{T}_5^+$, $\bar{T}_6^+$; (ii) the stable modes are also zero at the wall; (iii) the fundamental mode $\bar{T}_1$ has a single maximum between the axis and the wall; (iv) the stable harmonics $n = 2, 3, 4$ have n maxima and $n - 1$ zeros.

Thus besides the unstable diverging spectra, there are three kinds of stable spectra for the fundamental mode $n = 1$ (first three harmonics $n = 2, 3, 4$): (i) monotonic (oscillatory) decay for the dimensionless radial (Figure 4) and azimuthal (Figure 5) velocity perturbation spectra, that are non-zero on axis and zero at the wall; (ii) non-zero at the wall for the dimensionless mass density (Figure 6) and pressure (Figure 8) perturbation spectra with a single dip (n dips and $n - 1$ maxima); (iii) zero on axis and at the wall for the dimensionless entropy (Figure 7) and temperature (Figure 9) perturbation spectra with a single maximum (n maxima and $n - 1$ zeros).

7. DISCUSSION

The present paper may be the first to combine the interactions of the three types of waves in a fluid not subject to external force fields, hence the designation acoustic-vortical-entropy (AVE) waves. A deliberate choice was made of one of the simplest baseline flows that could support AVE waves, namely an incompressible non-isentropic uniform flow with rigid body swirl, leading to a mean flow pressure and sound speed varying radially due to the centrifugal force. The linear non-dissipative perturbation of this mean flow leads in the axisymmetric case to the AVE wave equations (25;26a-c) first obtained here. The exact solution is obtained in terms of Gaussian hypergeometric functions in the case of zero axial wavenumber, when there is only temporal and radial dependences.

An important feature of the problem is the existence of a critical layer where the swirl velocity equals the

$0 \le r \le r_1$	$r_1 = 0.4r_0$	$r_1 = 0.8r_0$	$r_1 = 1.2r_0$	$r_1 = 1.6r_0$
κ_1	9.874	5.322	3.895	3.217
κ_2	18.015	9.626	6.974	5.700
κ_3	26.103	13.920	10.061	8.203
κ_4	34.175	18.212	13.150	10.712
κ_5	42.240	22.502	16.241	13.027±i14.338
κ_6	50.302	26.791	18.195±i27.868	15.588±i7.640

Table 2: First six eigenvalues of the radial wavenumber for acoustic-vortical-entropy waves in a cylinder $0 \le r \le r_1$ with rigid wall with radius r_1 a fraction of the critical radius.

$0 \le r \le r_1$	$r_1 = 0.4r_0$	$r_1 = 0.8r_0$	$r_1 = 1.2r_0$	$r_1 = 1.6r_0$
$\bar{\omega}_1$	10.110	5.748	4.460	3.881
$\bar{\omega}_2$	18.145	9.868	7.304	6.100
$\bar{\omega}_3$	26.193	14.089	10.293	8.485
$\bar{\omega}_4$	34.244	18.341	13.329	10.930
$\bar{\omega}_5$	42.296	22.606	16.386	13.109±i14.248
$\bar{\omega}_6$	50.349	26.879	18.234±i27.809	15.710±i7.581

Table 3: As the Table 2 for the corresponding values of the dimensionless frequency.

isothermal sound speed. It is shown that this condition of isothermal swirl Mach number unity corresponds to a finite wave field, and thus is a singularity of the AVE wave equation but not a singularity of the wave field. The linear non-dissipative non-isentropic compressible vortical perturbations of the non-isentropic uniform flow with rigid swirl may be interpreted alternatively as (i) acoustic-vortical entropy (AVE) waves or (ii) stability or instability modes of the mean flow. This dual interpretation is demonstrated for a cylindrical duct with rigid wall at the radius $a = 1.6r_0$, that is 60% larger than the critical layer, for: (a) the eigenvalues for the wavenumber (Table 2) and frequency (Table 3); (b) the eigenfunctions for the radial (Figure 4) and azimuthal (Figure 5) velocity, mass density (Figure 6), entropy (Figure 7), pressure (Figure 8) and temperature (Figure 9). These confirm that the wave field is finite at the critical layer in this as well as in all other cases; in this particular case, the fundamental and first three harmonics are stable and the fifth and sixth harmonics are unstable. The general theory applies to all cases of cylindrical or annular ducts or cylindrical cavities containing or not the critical layer.
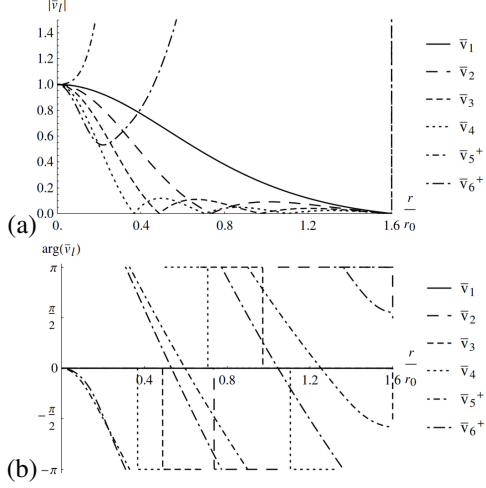
Figure 4: Modulus (top) and phase (bottom) versus radial distance normalized to the critical radius, for dimensionless radial velocity perturbation spectrum, of the first six modes of acoustic-vortical-entropy waves in a rigid cylinder with radius equal to 1.6 of the critical radius.
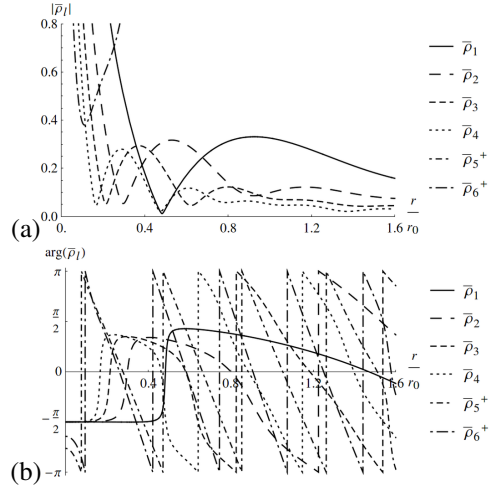
Figure 6: As of Figure 4 for the dimensionless mass density perturbation spectrum.
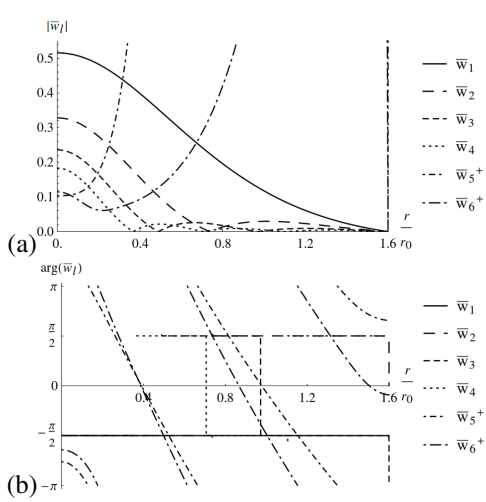
Figure 5: As of Figure 4 for the dimensionless azimuthal velocity perturbation spectrum.
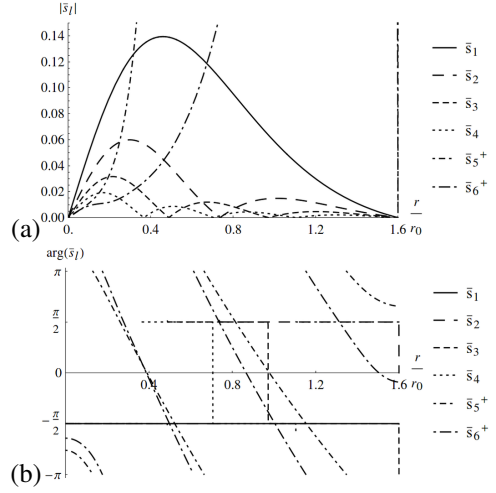
Figure 7: As of Figure 4 for the dimensionless entropy perturbation spectrum.

13
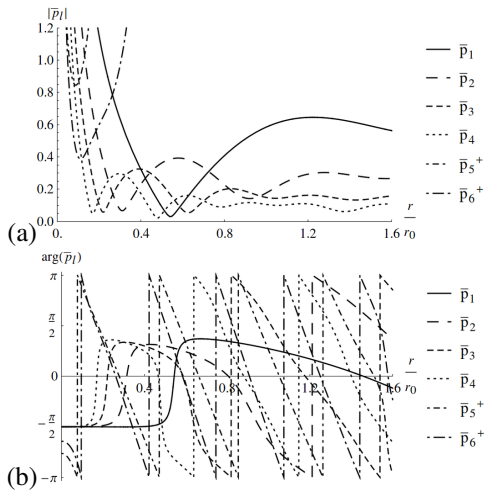
Figure 8: As of Figure 4 for the dimensionless pressure perturbation spectrum.
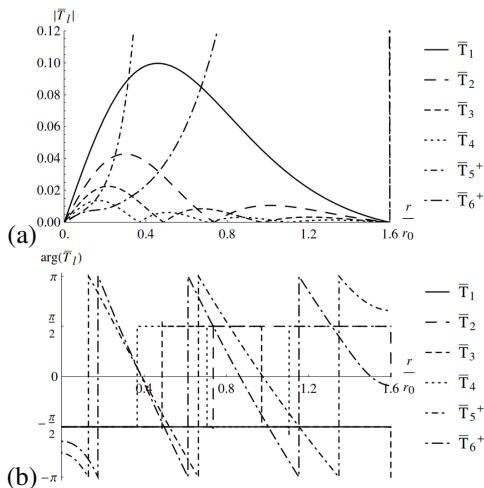
Figure 9: As of Figure 4 for the dimensionless temperature perturbation spectrum.

References

[1] A. D. Pierce, Acoustics: An Introduction to Its Physical Principles and Applications, McGraw-Hill, 1981, ISBN:9780883186121.

[2] L. M. B. C. Campos, On magnetoacoustic-gravity-inertial (MAGI) waves I. generation, propagation, dissipation and radiation, Mon Not R Astron Soc 410 (2) (2011) 717–734, doi:10.1111/j.1365-2966.2010.17553.x.

[3] J. Lighthill, Waves in Fluids, Cambridge Mathematical Library, Cambridge U.P., 1978, ISBN:9780521010450.

[4] L. M. B. C. Campos, Complex Analysis with Applications to Flows and Fields, Vol. 1 of Mathematics and Physics in Science and Engineering, CRC Press, 2010, ISBN:9781420071184.

[5] L. M. B. C. Campos, F. J. P. Lau, On sound generation by moving surfaces and convected sources in a flow, Int J Aeroacoust 11 (1) (2012) 103–136, doi:10.1260/1475-472X.11.1.103.

[6] L. M. B. C. Campos, On the generalizations of the doppler factor, local frequency, wave invariant and group velocity, Wave Motion 10 (3) (1988) 193–207, doi:10.1016/0165-2125(88)90018-2.

[7] L. M. B. C. Campos, On 24 forms of the acoustic wave equation in vortical flows and dissipative media, Appl Mech Rev 60 (6) (2007) 291–315, doi:10.1115/1.2804329.

[8] L. M. B. C. Campos, M. H. Kobayashi, On sound emission by sources in a shear flow, Int J Aeroacoust 12 (7-8) (2013) 719–742, doi:10.1260/1475-472X.12.7-8.719.

[9] L. M. B. C. Campos, P. G. T. A. Serrão, On the continuous and discrete spectrum of acoustic-vortical waves, Int J Aeroacoust 12 (7-8) (2013) 743–782, doi:10.1260/1475-472X.12.7-8.743.

[10] C. C. Lin, The Theory of Hydrodynamic Stability, Cambridge Monographs on Mechanics Applied Mathematics, Cambridge U.P., 1955, aSIN:B0000CJB1L.

[11] L. M. B. C. Campos, Transcendental Representations with applications to Solids and Fluids, Vol. 2 of Mathematics and Physics in Science and Engineering, CRC Press, 2012, ISBN:9781439834312.

[12] C. J. Heaton, N. Peake, Acoustic scattering in a duct with mean swirling flow, J Fluid Mech 540 (2005) 189–220, doi:10.1017/S0022112005005719.

[13] C. J. Heaton, N. Peake, Algebraic and exponential instability of inviscid swirling flow, J Fluid Mech 565 (2006) 279–318, doi:10.1017/S0022112006001698.

[14] E. L. Ince, Ordinary Differential Equations, Dover, 1956, ISBN:9780486603490.

[15] A. R. Forsyth, A Treatise on Differential Equations, Dover, 1929, ISBN:9780486693149.

[16] E. T. Whittaker, G. N. Watson, A Course of Modern Analysis, Cambridge UP, 1927, ISBN:9781603864541.

[17] C. Carathéodory, Theory of Functions of a Complex Variable, Vol. 1–2, Verlag Birkhauser, 1950, ISBN:9780821828311.

[18] M. Abramowitz, I. A. Stegun (Eds.), Handbook of mathematical functions, Vol. 55 of Dover Books on Advanced Mathematics, Dover, 1965, ISBN:9780486612720.

[19] T. Bromwich, T. M. MacRobert, An Introduction to the Theory of Infinite Series, MacMillan, 1926, ISBN:9781164810001.

[20] K. Knopp, Theory and Application of Infinite Series, Dover (reprint 1990, 1921, ISBN:9780486661650.